Influence of carrier density on the electronic cooling channels of bilayer graphene

T. Limmer, ¹ A. J. Houtepen, ² A. Niggebaum, ¹ R. Tautz, ¹ and E. Da Como ^{1,a)}
¹ Photonics and Optoelectronics Group, Physics Department and CeNS, Ludwig-Maximilians-Universität München, Amalienstrasse 54, 80799 München, Germany
² Chemical Engineering, Delft University of Technology, 2628 BL Delft, The Netherlands

(Received 5 July 2011; accepted 9 August 2011; published online 9 September 2011)

We study the electronic cooling dynamics in a single flake of bilayer graphene by femtosecond transient absorption probing the photon-energy range 0.25–1.3 eV. From the transients, we extract the carrier cooling curves for different initial temperatures and densities of the photoexcited electrons and holes. Two regimes of carrier cooling, dominated by optical and acoustic phonons emission, are clearly identified. For increasing carrier density, the crossover between the two regimes occurs at larger carrier temperatures, since cooling via optical phonons experiences a bottleneck. Acoustic phonons, which are less sensitive to saturation, show an increasing contribution at high density. © 2011 American Institute of Physics, [doi:10.1063/1.3633099]

The dynamics of carrier cooling is of particular interest in carbon based low dimensional structures, such as carbon nanotubes and graphene, because of their extraordinary mobilities and current densities in devices, in the presence of strong electron-phonon interactions.² Hot carriers are expected to emit optical phonons as long as their energy with respect to the bottom of the band is above the optical phonon energy $\hbar\Omega_{\rm op}$ (~195 meV G-mode in graphene). In proximity to this energy, acoustic phonons are the dominant cooling channel for equilibrating the electronic system with the lattice. Acoustic phonons are also responsible for the decay of the emitted optical phonons via anharmonic interactions.³ We consider the carrier cooling in bilayer graphene since this material is gaining an increasing interest in photonics and optoelectronics, where it can be used in photodiodes⁴ and lasers.⁵ It is, therefore, crucial to understand how hot carriers lose energy in different regimes of photocarrier density. In addition, the physics of cooling has triggered a considerable interest from the perspective of theoretical modeling, 6,7 but has seen limited experimental investigations, mainly focused on an epitaxial graphene.8

In this letter, we present the experimental determination of the carrier cooling rates in a single flake of bilayer graphene at photocarrier densities differing by one order of magnitude ($\sim 10^{11}$ to 10^{12} cm⁻²). The experiments are performed by means of femtosecond pump-probe spectroscopy in a previously unexplored broad probe photon-energy range, 0.25–1.3 eV, thus reflecting the dynamics of electron and hole populations each with half the photon-energy (0.125–0.65 eV). This range, which is below $\hbar\Omega_{\rm op}$, is expected to be sensitive to acoustic cooling. Modeling of the differential transmission spectra, $\Delta T/T$, allows us to extract the carrier temperatures as a function of time (cooling curves). Those reveal two regimes in which carriers first lose most of their energy via emission of optical phonons and, subsequently, via low energy acoustic. The crossover

between the two mechanisms depends on the carrier density and occurs at higher temperatures when the density is high.

Bilayer graphene flakes were prepared by mechanical exfoliation of natural graphite. The homogeneity and the number of layers were checked by micro-Raman. Single homogenous bilayer graphene flakes were then transferred to CaF_2 substrates to perform optical experiments (Fig. 1(a)). Carriers were photoexcited with 100 fs pulses at 1.55 eV from an amplified Ti:sapphire laser. Probe pulses with similar time durations were obtained from an optical parametric amplifier. Pump and probe beams were focused on a single flake in ambient conditions to detect $\Delta T(t,\hbar\omega)/T(\hbar\omega)$ at different photon energies, $\hbar\omega$, and time delays between the pump and the probe, t. Experiments were conducted in a linear regime between pump fluence and $\Delta T/T$ signal in the

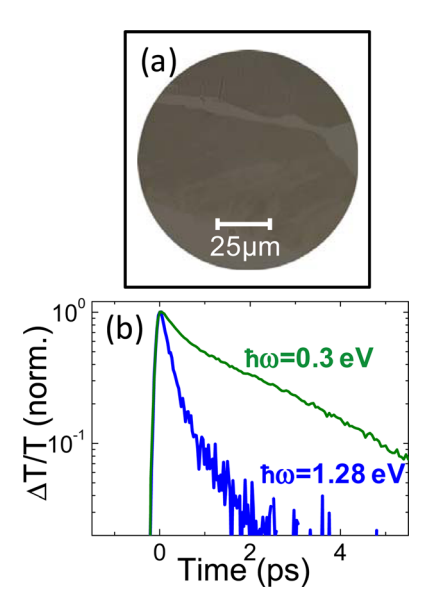


FIG. 1. (Color online) (a) Optical transmission microscopy image of the bilayer graphene sample. (b) Normalized differential transmission transients at probe energies 1.28 eV and 0.30 eV; photocarrier density of $5.0 \times 10^{11} \, \mathrm{cm}^{-2}$.

a) Author to whom correspondence should be addressed. Electronic mail: enrico.dacomo@physik.uni-muenchen.de.

probe energy range 0.6–1.3 eV, suggesting a minor contribution from Auger effects.

Figure 1(c) shows the $\Delta T/T$ transients at 1.28 and 0.3 eV. While we observe an almost monoexponential decay of \sim 4 ps at 0.3 eV, at high energy, the dynamics exhibits a faster decay of 500 fs. This shows how carrier relaxation is strongly dependent on the choice of the optically coupled states investigated by the probe. To have a more complete picture of the carrier dynamics, we report, in Figure 2, $\Delta T(\hbar\omega)/T(\hbar\omega)$ spectra at different t. At t=0, a positive $\Delta T/T$ is detected across the whole energy range investigated. For both densities of carriers, the signal amplitude is monotonically decreasing towards energies closer to the pump (1.55 eV). This is clearly different from results reported in the previous optical experiments on epitaxial graphene. 8,10,11 In such samples, the substrate induced doping gives rise to negative $\Delta T/T$ signals (absorption) at the Fermi edge, which is shifted by up to 300 meV from the Dirac-point. 11 A positive $\Delta T/T$ over the whole spectral range investigated, as reported in our experiments, is due to state filling of the optically coupled states and gives direct access to the relaxation of carriers. At low carrier density (Fig. 2(a)), the delayed spectra recorded at 0.5 and 2.5 ps exhibit an almost vanishing signal on the high photon-energy part, whereas between 0.25 and 0.5 eV, the $\Delta T/T$ remains with a non-negligible amplitude, indicating that carriers in this energy range are blocking the interband transitions with a slower decay. These results demonstrate that upon photoexcitation, a fast cooling of the carriers at photon energies closer to the pump occurs. In Figure 2(b), we show the transient spectra for a higher excitation density, corresponding to 1.8×10^{12} cm⁻². Here, the spectra at 0.5 and 2.5 ps are characterized by slowly decaying dynamics extending to 1.0 eV, suggesting that also carriers populating states at energies closer to the pump have a longer lifetime.

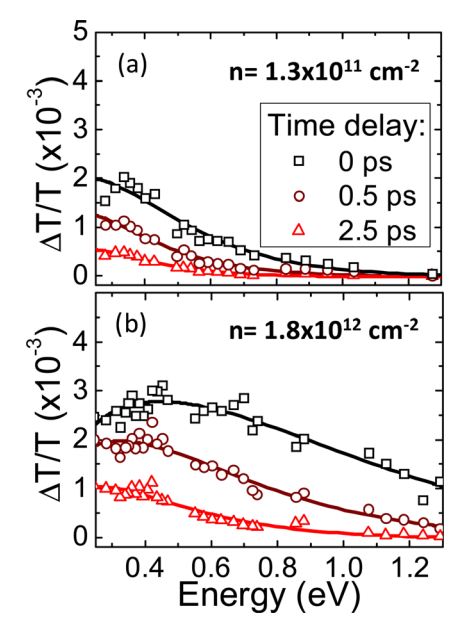


FIG. 2. (Color online) Differential transmission spectrum of bilayer graphene for three time delays (0 ps: black squares, 0.5 ps: brown circles, and 2.5 ps: red triangles) between pump and probe for photocarrier densities of (a) $1.3 \times 10^{11} \text{cm}^{-2}$ and (b) $1.8 \times 10^{12} \text{cm}^{-2}$. The solid lines are fits according to the model.

To extract the carrier temperatures, we have fitted the $\Delta T(t,\hbar\omega)/T(\hbar\omega)$ data with a model considering two Fermi-Dirac distributions, for electrons and holes, characterized by a carrier temperature T_c and two separated chemical potentials. Such a description have been demonstrated to be the most appropriate for the ultrafast dynamics of carriers in graphite. The transient absorption ΔA is modeled considering the difference in the excited and ground state dynamical conductivities, σ_{ex}^{tot} and σ_{gr}^{tot} .

$$\Delta A \propto -\ln(1 + \Delta T) \cong -\Delta T$$
, $|\Delta T| \ll 1$

$$\frac{\Delta T}{T} \cong -\frac{4\pi}{c} (\sigma_{ex}^{tot} - \sigma_{gr}^{tot}) A_0,$$

where σ^{tot} is the sum of the inter- and intra-band contributions.

$$\sigma^{tot}(T_C, \hbar\omega) = \sigma^{inter}(T_C, \hbar\omega) + \sigma^{intra}(T_C, \hbar\omega).$$

The intraband contribution is a Drude-like term from Ref. 13 used to account for the slight decrease in $\Delta T/T$ on the low energy side of the spectra at high carrier density (cf. Fig. 2(b)). A_o is the ground state absorption, which is constant in the probed range, ¹⁴ while T_C and the chemical potential are used as fitting parameters. The model assumes that the ultrafast carrier-carrier scattering, occurring in less than 10 fs, ¹² results in two Fermi-Dirac populations, with a common characteristic temperature T_C . This is established within the time resolution of our measurements (\sim 150 fs). The subsequent decrease in carrier population in the high energy tails of the spectra is due to carrier-phonon scattering and eventually recombination.

The fits shown as solid lines in Figs. 2(a) and 2(b) reproduce well the recorded experimental curves through the whole photon energy range investigated. The cooling curves are plotted in Fig. 3, for four different initial densities of carriers. All curves show an initial fast decrease consistent with the emission of optical phonons, followed by a longer tail due to coupling with acoustic. From here it is possible to extract the energy loss rate (power loss) $P = \partial(k_B T_C)/\partial t$ at different Tc and carrier densities. Figure 4 shows the logarithm of the energy loss rate versus the inverse carrier temperature $1/k_B T_C$. P is decreasing with carrier temperature

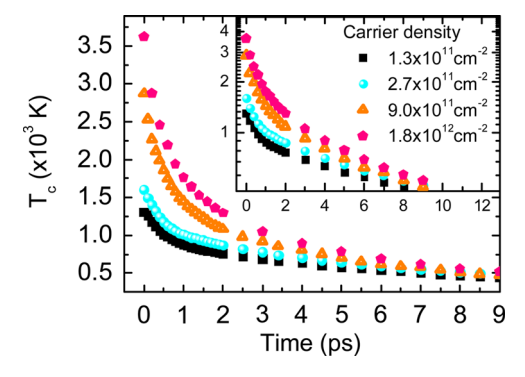


FIG. 3. (Color online) T_c as a function of time for four different carrier densities as specified in the legend. The inset shows the same cooling curves on a logarithmic temperature scale.

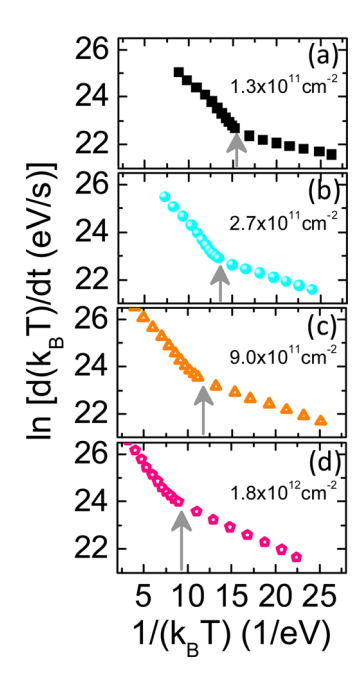


FIG. 4. (Color online) Logarithm of the energy loss rate $\partial(k_BT_C)/\partial t$ as a function of $1/T_c$ for the carrier densities (a) $1.3 \times 10^{11} {\rm cm}^{-2}$, (b) $2.7 \times 10^{11} {\rm cm}^{-2}$, (c) $9.0 \times 10^{11} {\rm cm}^{-2}$, and (d) $1.8 \times 10^{12} {\rm cm}^{-2}$. The arrows indicate the turning point between a cooling mechanism dominated by optical phonons and acoustic phonons.

exhibiting two clearly distinct regimes. In the initial regime, the power loss is expected to be dominated by the emission of optical phonons, while at lower temperatures, carriers can relax via low energy acoustic.⁶ The slopes of the curves in Fig. 4 are proportional to the energy of the phonons involved in P, since $P \cong \frac{\hbar\Omega}{L} e^{-\hbar\Omega/k_BT}$. A sum of the optical and acoustic cooling rates contributes to the overall P curve. ¹⁶ We report slopes of 350, 435, 424, 506 meV as a function of increasing carrier density for the initial regime and ~ 100 meV for the second. While 100 meV is in good agreement with the recent calculations on acoustic modes in graphene,³ the slopes of the initial regime is above the sum of the phonon energies and points to an additional carrier-dependent channel. Interestingly, the turning point towards the regime where cooling dynamics via acoustic phonons is dominant clearly depends on the carrier density (arrows). One can explain this behavior considering that the power loss is proportional to the carrier temperature and density for both optical and acoustic cooling.^{6,7} However, optical phonons once excited transfer their energy to acoustic modes and from there to the heat bath. The transfer from optical to acoustic may not be as efficient as carrier optical-phonon transfer leading to a large population of optical phonons and decreased cooling rate, *hot phonon effect*. The hot phonon effect is less apparent in the cooling via acoustic modes, since those have a lower thermal-impedance mismatch with the heat bath. We suggest that in the presence of the *hot phonon effect*, cooling via acoustic phonons takes place already at higher Tc.

In conclusion, we have measured the cooling rate of photoexcited carriers in a flake of bilayer graphene as a function of carrier density. At high T_C , above 1000 K, the cooling occurs via emission of optical phonons which increase rapidly their population and leads to a hot phonon effect. This process is less pronounced in the cooling via acoustic phonons, since those are faster thermalized with the heat bath.

This work has been supported by the Deutsche Forschungsgemeinschaft (DFG) via the excellence cluster Nanosystems Initiative Munich (NIM).

¹J. C. Tsang, M. Freitag, V. Perebeinos, J. Liu, and P. Avouris, Nat. Nanotechnol. **2**, 725 (2007).

²A. Gambetta, C. Manzoni, E. Menna, M. Meneghetti, G. Cerullo, G. Lanzani, S. Tretiak, A. Piryatinski, A. Saxena, R. L. Martin, and A. R. Bishop, Nat. Phys. **2**, 515 (2006).

³N. Bonini, M. Lazzeri, N. Marzari, and F. Mauri, Phys. Rev. Lett. **99**, 176802 (2007).

⁴T. Mueller, F. N. A. Xia, and P. Avouris, Nat. Photonics 4, 297 (2010).

⁵Z. P. Sun, T. Hasan, F. Torrisi, D. Popa, G. Privitera, F. Q. Wang, F. Bonaccorso, D. M. Basko, and A. C. Ferrari, ACS Nano 4, 803 (2010).

⁶W. K. Tse and S. Das Sarma, Phys. Rev. B **79**, 235406 (2009).

⁷R. Bistritzer and A. H. MacDonald, Phys. Rev. Lett. **102**, 206410 (2009).

⁸D. Sun, Z. K. Wu, C. Divin, X. B. Li, C. Berger, W. A. de Heer, P. N. First, and T. B. Norris, Phys. Rev. Lett. **101**, 157402 (2008).

⁹See supplementary material at http://dx.doi.org/10.1063/1.3633099 for description of the model, Raman and transmission spectra and experimental setup.

¹⁰H. N. Wang, J. H. Strait, P. A. George, S. Shivaraman, V. B. Shields, M. Chandrashekhar, J. Hwang, F. Rana, M. G. Spencer, C. S. Ruiz-Vargas, and J. Park, Appl. Phys. Lett. 96, 081917 (2010).

¹¹D. Sun, C. Divin, C. Berger, W. A. de Heer, P. N. First, and T. B. Norris, Phys. Rev. Lett. **104**, 136802 (2010).

¹²M. Breusing, C. Ropers, and T. Elsaesser, Phys. Rev. Lett. **102**, 086809 (2009).

¹³K. F. Mak, M. Y. Sfeir, Y. Wu, C. H. Lui, J. A. Misewich, and T. F. Heinz, Phys. Rev. Lett. **101**, 196405 (2008).

R. R. Nair, P. Blake, A. N. Grigorenko, K. S. Novoselov, T. J. Booth, T. Stauber, N. M. R. Peres, and A. K. Geim, Science 320, 1308 (2008).

¹⁵S. Butscher, F. Milde, M. Hirtschulz, E. Malic, and A. Knorr, Appl. Phys. Lett. **91**, 203103 (2007).

¹⁶S. Das Sarma, J. K. Jain, and R. Jalabert, Phys. Rev. B 37, 6290 (1988).